http://dx.doi.org/10.5012/bkcs.2012.33.8.2529

Facile Coating of Poly(3,4-ethylenedioxythiophene) on Manganese Dioxide by Galvanic Displacement Reaction and Its Electrochemical Properties for Electrochemical Capacitors

Kwang-Heon Kim, Ji-Young Kim, and Kwang-Bum Kim*

*Department of Material Science and Engineering, Yonsei University, Seoul 120-749, Korea. *E-mail: kbkim@yonsei.ac.kr*
Received May 1, 2012, Accepted May 1, 2012

Poly(3,4-ethylenedioxythiophene) coated Manganese Dioxide (PEDOT/MnO_2) composite electrode was fabricated by simply immersing the MnO_2 electrode in an acidic aqueous solution containing 3,4-ethylenedioxythiophene (EDOT) monomers. Analysis of open-circuit potential of the MnO_2 electrode in the solution indicates the reduction of outer surface of MnO_2 to dissolved Mn^{2+} ions and simultaneously oxidation of EDOT monomer to PEDOT on the MnO_2 surface to form a PEDOT shell *via* a galvanic displacement reaction. Analysis of cyclic voltammograms and specific capacitance of the PEDOT/MnO_2, conductive carbon added MnO_2 and conductive carbon added PEDOT/MnO_2 electrodes suggests that the conductive carbon acted mainly to provide a continuous conducting path in the electrode to improve the rate capability and the PEDOT layer on MnO_2 acts to increase the active reaction site of MnO_2.

Key Words : MnO_2, PEDOT, Galvanic displacement reaction, Electrochemical capacitor

Introduction

Manganese dioxide (MnO_2) has been reported as a promising electroactive material for energy storage devices because of its high energy density, low cost, environmental friendliness, and natural abundance.[1] In particular, electrochemical capacitors employing the MnO_2 as electroactive materials have been investigated since the first report on faradic pseudocapacitive behaviors of amorphous MnO_2 in KCl solution by Lee and Goodenough in 1999.[2]

Because of poor electronic conductivity of MnO_2, a relatively large amount of conductive carbon (10-30 wt %) is always included in MnO_2-based electrodes in order to make electrical contacts among the active material and between the active material and a current collector.[3,4] However, physical mixing of MnO_2 and the conductive carbon would form a limited number of electrical contacts, which results in electrochemical reaction taking place in the vicinity of these contacts and reduces the electrochemical utilization of the active material. Recently, MnO_2/carbon (ex. carbon black, carbon nanotube and graphene) nanocomposites prepared by coating MnO_2 on the surface of the nanocarbon have been investigated in order to increase the electrical conductivity of MnO_2 electrode.[5,6] However, electrical contact among the MnO_2/carbon nanocomposites still remains a problem as the MnO_2 loading is increased in the composites, because the carbon core becomes coated with a thicker MnO_2 layer and ceases to provide a conductive path in the composites. From the view of the electrical conductivity, the conductive carbon should make electrical contacts among active material and provide a continuous conducting path in the electrode.

For this reason, coating of MnO_2 particles with a thin conductive layer that is permeable to ions might be very advantageous to the improvement of electrochemical utilization of the active material.

Poly(3,4-ethylenedioxythiophene) (PEDOT) is a most promising conducting polymer due to its good electrical conductivity (~600 Scm^{-1}) and good environmental stability among other polymers.[7] Recently, studies on the synthesis of PEDOT coated MnO_2 have been reported in order to improve the electrochemical utilization and high rate capability.[8,9]

Electrochemical or chemical polymerization of monomer using a soluble oxidizing agent has been widely used for the preparation of conducting polymer coated metal oxides.[9-11] Although an electrochemical method is fast and reliable, it requires a fabrication of a metal oxide electrode and an external power supply for the electrochemical polymerization. On the other hand, chemical method, which usually requires a soluble oxidizing agent for oxidative polymerization of a monomer, suffers from difficulties in controlling the morphology and thickness of a conducting polymer on the surface of oxide on the nanometer scale. Furthermore, it is highly likely to have an unwanted separate polymerization within a solution away from the metal oxide. Previously, chemical oxidation of pyrrole into polypyrrole in the presence of α-MnO_2, β-MnO_2 or spinel $LiMn_2O_4$ without using any soluble oxidizing agents was reported.[12] Ali H. Gemeay *et al.* reported on the preparation of polyaniline/MnO_2 composites by using β-MnO_2 as an oxidant in an aniline solution.[13]

Galvanic displacement reaction has been extensively used for the synthesis of metallic core/shell nanostructures such as Co/Au, Co/Cu, and Au/Ag nanoparticles,[14,15] in which the metallic core was used as a reducing agent as well as a

sacrificial template. It is a spontaneous process which involves the reduction of ions of a more noble metal along with a simultaneous oxidation of a less noble metal driven by a difference in redox potentials of two redox couples. Since the electrochemical reactions involved in the chemical oxidation of the monomers in the presence of manganese oxides without using any soluble oxidizing agents are analogous in nature to those for the galvanic displacement reaction of the metallic core/shell nanostructures, analysis of a chemical polymerization process from a view of the galvanic displacement reaction would offer an insight into for the synthesis of a conducting polymer coated oxide.

In this study, we report on the preparation of composite electrodes composed of PEDOT coated MnO_2 particles using a galvanic displacement reaction between MnO_2 and 3,4-ethylenedioxythiophene (EDOT) monomers in an acidic aqueous solution and the analysis of their electrochemical properties for electrochemical capacitor applications considering the roles of a conductive carbon and PDEOT layer coated on MnO_2 in the composite electrodes.

Experimental

MnO_2 was prepared by a redox reaction of MnO_4^- and Mn^{2+} in an aqueous solution according to the following reaction: $2MnO_4^- + 3Mn^{2+} + 2H_2O \rightarrow 5MnO_2 + 4H^+$.[2] Briefly, a mixture of 40 mL of 0.1 M $KMnO_4$ solution and 60 mL of 0.1 M $MnSO_4$ solution were reacted at room temperature for 12 h. A dark-brown precipitate was filtered, repeatedly washed with deionized water, and then dried at 100 °C in air for 12 h.

MnO_2 electrode without conductive carbon (denoted as a MnO_2 electrode) was prepared by mixing 90 wt % MnO_2 and 10 wt % polyvinylidene fluoride (PVDF) dissolved in *N*-methylpyrrolidone as a binder. MnO_2 electrode with conductive carbon (denoted as a C-MnO_2 electrode) was prepared by mixing 70 wt % MnO_2, 20 wt % acetylene black and 10 wt % PVDF. The slurry mixture was coated on a Ni foam substrate and then dried at 100 °C for overnight. The electrode with a 1 × 1 cm^2 area contained 4-5 mg of the dried slurry.

For PEDOT coating, an acidic EDOT monomer solution was prepared by mixing 40 mL of 0.01 M EDOT aqueous solution with 2 mL of 1M H_2SO_4 under stirring at room temperature for 2 h. The PEDOT coated MnO_2 (denoted as a PEDOT/MnO_2) and PEDOT coated C-MnO_2 (denoted as a PEDOT/C-MnO_2) electrodes were prepared by immersing the MnO_2 electrode and the C-MnO_2 electrode in the acidic EDOT solution for 10-120 sec. For comparison purposes, a PEDOT electrode was prepared on a Ni foam substrate by an electrochemical polymerization using potential cycling in a solution of 0.01 M EDOT and 0.025 M $LiClO_4$.

To monitor the galvanic displacement reaction between MnO_2 and EDOT, open circuit potential (OCP) of the MnO_2 electrode was measured in an acidic solution containing EDOT monomers. The OCP measurements were made in a two-electrode cell at room temperature. The working and reference electrodes were the MnO_2 electrode and the saturated calomel electrode (SCE), respectively. X-ray diffraction (XRD) measurements were carried out with a Regaku Rint-2000 instrument using Cu-Kα radiation (λ = 1.54178 Å). Raman spectra were measured on a Jobin-Yvon T64000 spectrophotometer (excitation radiation = 514.532 nm). The morphology was characterized by transmission electron microscopy (TEM, JEOL JEM2100F) and scanning electron microscope (SEM, Hitachi S-4300SE). The TEM was equipped with an energy dispersive X-ray spectrometer (EDS).

Cyclic voltammetry (CV) was performed in 1 M Na_2SO_4 aqueous solution within a potential window of 0.0 to 0.8 V_{SCE} using a three-electrode cell equipped with the MnO_2 working electrode, the platinum mesh counter electrode, and the SCE reference electrode and a potentiostat/galvanostat (VMP2, Princeton Applied Research).

Results and Discussion

Figure 1(a, b) shows the SEM images of the MnO_2 and PEDOT/MnO_2 composites prepared in this study. In Figure 1(a), the MnO_2 before PEDOT coating is in the form of agglomerated MnO_2 cluster composed of spherical particles with diameters ranging from 200 to 300 nm and fairly rough surface. Upon the immersion of the MnO_2 electrode into the EDOT monomer solution, all the MnO_2 particles were uniformly coated with PEDOT while maintaining the initial spherical morphology as shown in Figure 1(b). It is worth noting that no free PEDOT particles were found in numerous SEM analyses of the PEDOT/MnO_2 composites.

TEM image of the PEDOT/MnO_2 composites in Figure 1(c) clearly shows a 20 nm-thick layer of PEDOT coated on the spherical MnO_2 particles for an immersion time of 120 sec. Strong C, O, and S signals in EDS spectrum taken in the outermost layer of the PEDOT/MnO_2 composite (Fig. 1(c))

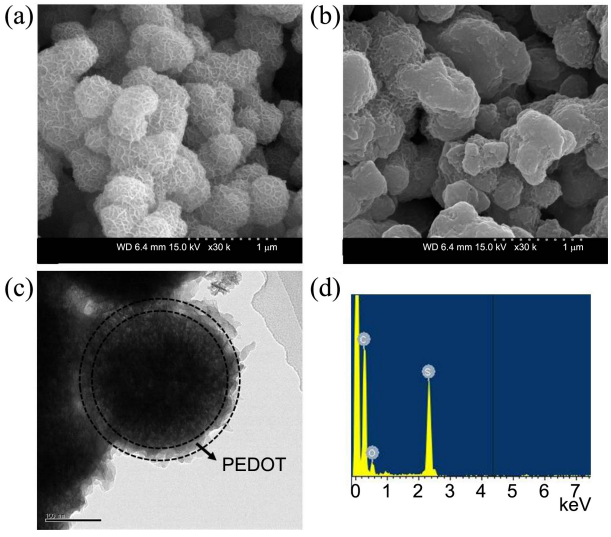

Figure 1. SEM images of (a) MnO_2, (b) PEDOT/MnO_2, (c) TEM image of PEDOT/MnO_2 and (d) EDS spectra taken from thin layer on MnO_2 in TEM image (Fig. (c))

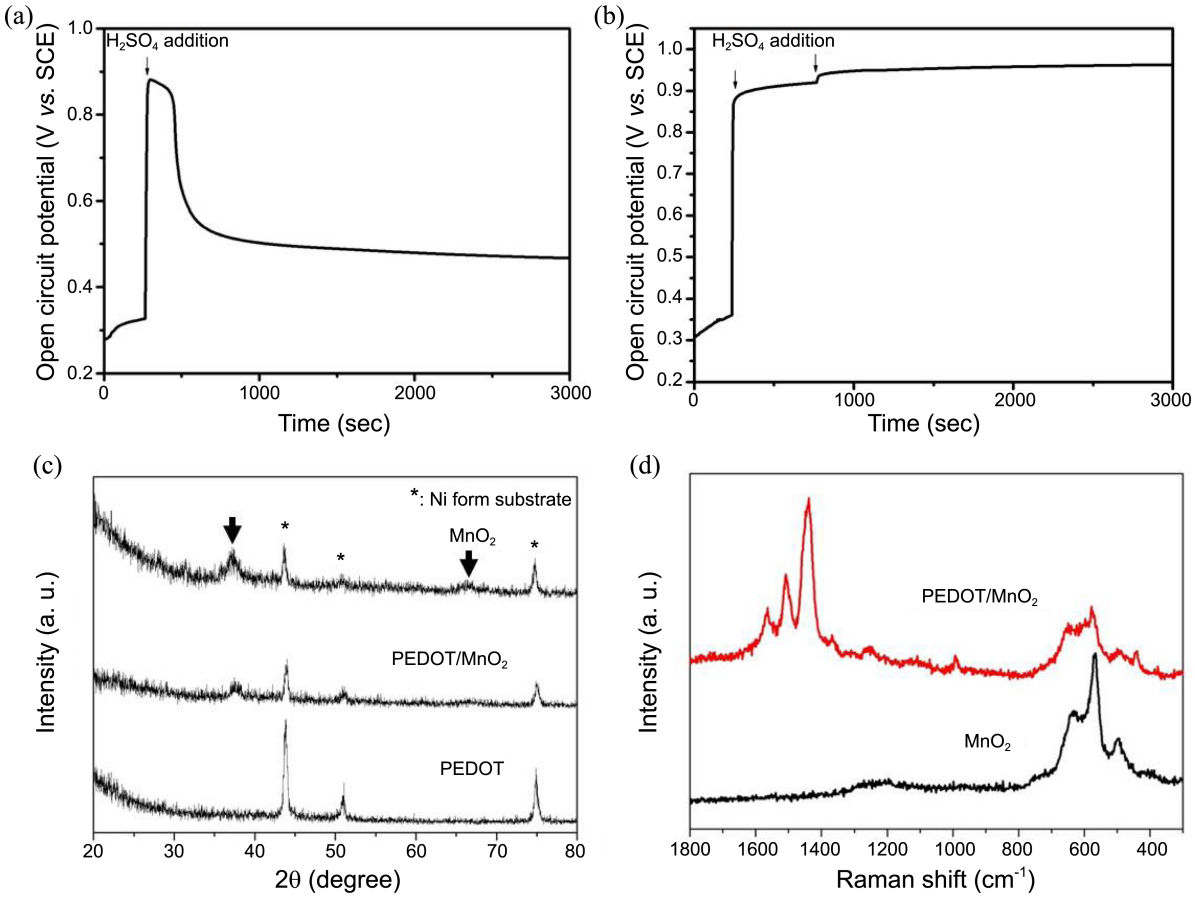

Figure 2. Open circuit potential-time profile of (a) MnO_2 electrode in 0.01 M EDOT solution, (b) MnO_2 electrode in an acidic solution without EDOT, (c) XRD patterns of MnO_2, PEDOT/MnO_2 and PEDOT and (d) Raman spectra of MnO_2 and PEDOT/MnO_2.

confirms that PEDOT was coated on the surface of MnO_2 (Fig. 1(d)). It indicates that the oxidative polymerization of EDOT was predominantly occurred on the outer surfaces of MnO_2.

Since the redox potentials of MnO_2/Mn^{2+} and EDOT/PEDOT are 1.2 V_{SHE}[16] and 1.0 V_{SHE},[17] the galvanic displacement reaction is likely to occur due to a difference in the redox potentials between MnO_2 and EDOT monomer. In order to investigate the galvanic displacement reaction between MnO_2 and EDOT, the open-circuit potential (OCP) of the MnO_2 electrode was measured in an acidic solution containing EDOT monomers. Figure 2(a) shows the change in the OCP of the MnO_2 electrode in the solution as a function of time. Initially, the OCP of the MnO_2 electrode was 0.3 V. Upon the addition of 1 M H_2SO_4, the potential instantly jumped to 0.88 V due to a rapid decrease in pH in the first stage.[16] Right after the sharp increase in OCP, a potential plateau was observed around 0.85 V for 200 sec in the second stage. This potential is similar to that observed in an electrochemical polymerization of EDOT using a galvanostatic technique.[18] It suggests that the reaction occurring around 0.85 V in the second stage could be an oxidative polymerization of EDOT coupled with a simultaneous reduction of MnO_2 by the galvanic displacement reaction. During the second stage, dark-brown MnO_2 turned to deep-blue indicating the formation of PEDOT on the surface of MnO_2. The amount of PEDOT coating in composites could be controlled depending on the reaction time in the second stage. For comparison, the OCP of MnO_2 electrode was measured in an acidic solution without EDOT. It was 0.95 V (Fig. 2(b)). Little variation of the OCP was observed with time in both cases and it indicates that no chemical reaction occurred to change a redox state of an interface between the MnO_2 and the solutions. In the third stage, the OCP decreased rapidly and gradually approached to 0.4 V, which is close to the OCP of a pure PEDOT electrode in an acidic solution. Analysis of the OCP suggests the polymerization of EDOT on MnO_2 in an acidic solution is due to the galvanic displacement reaction taking place between MnO_2 and EDOT. Little difference was observed in the OCP-time profiles of the MnO_2 electrode and the C-MnO_2 electrode in the acidic EDOT solution.

Figure 2(c) shows the XRD patterns of the MnO_2, PEDOT/MnO_2 and PEDOT electrodes. The MnO_2 electrode exhibited a poorly resolved diffraction pattern with two broad peaks at approximately 37° and 66° which correspond to MnO_2. MnO_2 prepared by a redox reaction of MnO_4^- and Mn^{2+} was reportedly to have the nanocrystalline nature with poor crystallinity.[19] During the galvanic displacement reaction between MnO_2 and EDOT, reduction of MnO_2 might pro-

duce the reduced phases of MnO_2 such as Mn_2O_3, MnOOH, Mn_3O_4, and $Mn(OH)_2$ which are commonly observed in the chemical reduction of MnO_2.[20] However, the XRD pattern of the PEDOT/MnO_2 electrode was similar to that of MnO_2 electrode before PEDOT coating and no reduced phases of MnO_2 were found in the XRD pattern of the PEDOT/MnO_2 electrode. Due to amorphous nature of PEDOT, no PEDOT diffraction peaks were observed for the PEDOT/MnO_2 electrode (Fig. 2(c)).

Figure 2(d) shows the Raman spectra of the MnO_2 and PEDOT/MnO_2 electrodes, respectively. The Raman spectrum of the MnO_2 is dominated by three bands at 497, 567, and 633 cm^{-1}, respectively. This feature is close to that of a birnessite-type MnO_2.[21] Raman spectrum of the PEDOT/MnO_2 clearly shows the characteristic bands at 1507, 1444, 1367 and 1253 cm^{-1} corresponding to PEDOT.[22] It should be noted that the characteristic bands of the birnessite-type MnO_2 was retained in the composites, which confirms that the galvanic displacement reaction between MnO_2 and EDOT did not cause any phase transformation of MnO_2.

Figure 3(a) shows CVs of the MnO_2 and PEDOT/MnO_2 electrodes prepared with different PEDOT coating time in the second stage of Figure 1 (10, 20, 30, 60, and 120 sec) at a potential scan rate of 2 mVs^{-1}. The MnO_2 electrode shows a distorted CV with a small current response mainly due to its low electrical conductivity of MnO_2 electrode. As PEDOT was coated on the MnO_2 electrode with an increase in the coating time up to 30 sec, CV of the PEDOT/MnO_2 electrode became gradually rectangular with an increase in current. With a further increase in the coating time up to 120 sec, the PEDOT/MnO_2 electrode showed a slight decrease in current while maintaining the rectangular-shaped CV. It suggests that the PEDOT coating on MnO_2 was very effective in improving the electrochemical utilization of MnO_2. The decrease in current observed for the PEDOT/MnO_2 electrodes for the PEDOT coating for 60 and 120 sec might be due to the loss of MnO_2 in the composite electrodes by the reduction of MnO_2 into dissolvable Mn^{2+} ions in the solution during the galvanic displacement reaction between MnO_2 and EDOT.

The specific capacitance was determined from the voltammetric charge of the CVs using the following equation:

$$C_s = \frac{q_a + |q_c|}{2m\Delta V}$$

where C_s, q_a, q_c, m, and ΔV are the specific capacitance, the anodic and cathodic voltammetric charges on the anodic and cathodic scans, the mass of the PEDOT/MnO_2 composite material, and the potential range of CV, respectively. Figure 3(b) shows the specific capacitances of the MnO_2 and the PEDOT/MnO_2 electrodes, which were calculated from the CVs at 2 mVs^{-1} as a function of the PEDOT coating time. As the PEDOT coating time was increased up to 30 sec, the specific capacitance increased linearly from 45 Fg^{-1} for the MnO_2 electrode to 134 Fg^{-1} (F per gram of PEDOT/MnO_2). When the coating time was further increased beyond 30 sec, the specific capacitance decreased slightly to 105 Fg^{-1} at

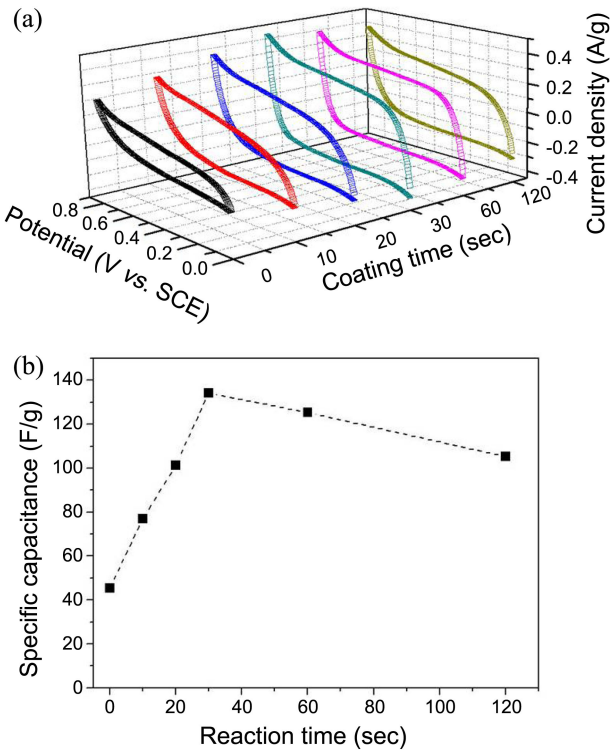

Figure 3. (a) CVs and (b) specific capacitance of MnO_2 and PEDOT/MnO_2 electrodes as a function of PEDOT coating time.

120 sec.

Analysis of Figure 3 suggests that the conductive PEDOT layer on MnO_2 provided an electron conduction path around the MnO_2 clusters, which resulted in an increase in the number of active reaction sites in the PEDOT/MnO_2 electrode compared with the MnO_2 electrode. The slight decrease in the specific capacitance of PEDOT/MnO_2 electrodes prepared for 60 and 120 sec from that for the composite electrode prepared for 30 sec might be due to the decrease in the amount of MnO_2 in the composites caused by the reduction of MnO_2 into dissolvable Mn^{2+} ions in the solution during the galvanic displacement reaction between MnO_2 and EDOT. It should be noted that MnO_2 reportedly shows a higher specific capacitance (100-150 Fg^{-1}) than PEDOT (~90 Fg^{-1}).[23,24]

Since the PEDOT/MnO_2 electrode with the coating time of 30 sec showed the highest specific capacitance, rate capability of the composite electrode was investigated for the following three electrodes: PEDOT/MnO_2 and C-PEDOT/MnO_2 electrodes with a coating time of 30 sec, and the C-MnO_2 electrode. Figure 4(a-e) show the CVs of the PEDOT/MnO_2, C-MnO_2 and PEDOT/C-MnO_2 electrodes measured at increasing potential scan rate from 2 mVs^{-1} to 100 mVs^{-1}. Each of the three electrodes showed a rectangular shaped CV and a similar current response at a low potential scan rate of 2 mVs^{-1}. As the potential scan rate was increased, a clear difference could be seen in the current response and shape of CV. The PEDOT/C-MnO_2 electrode and the C-MnO_2 electrode maintained the rectangular-shaped CVs up to the potential scan rate of 100 mVs^{-1}. And

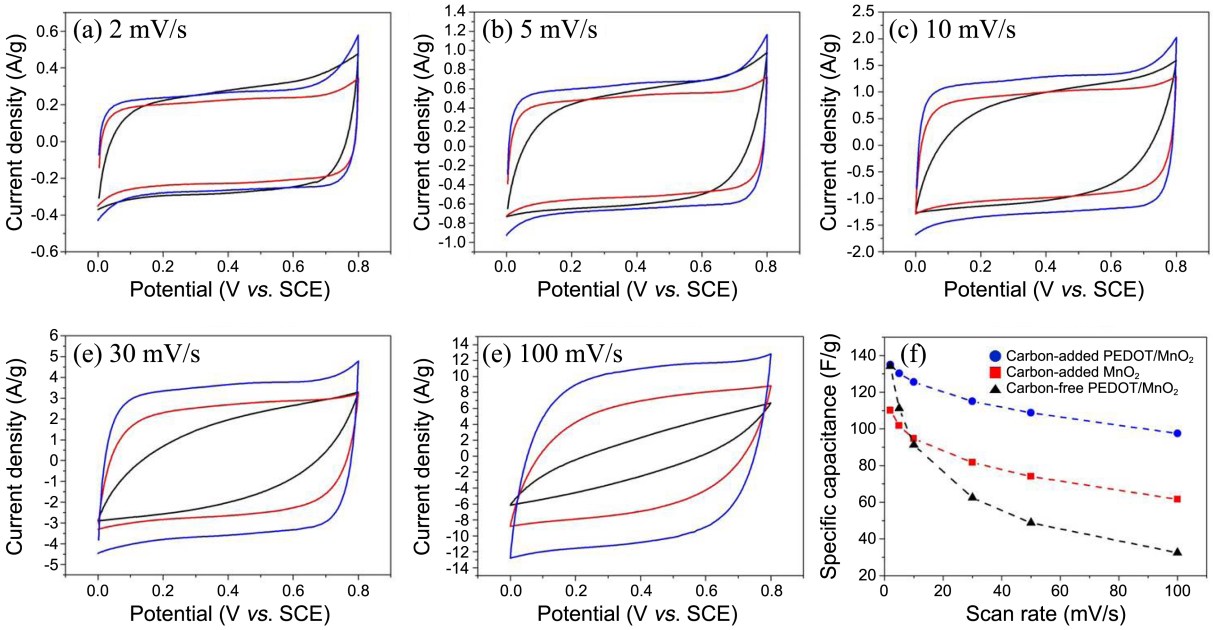

Figure 4. CVs of PEDOT/MnO_2, C-MnO_2 and PEDOT/C-MnO_2 electrodes as a function of potential scan rate. (a) 2, (b) 5, (c) 10, (d) 30 and (e) 100 mVs^{-1}. (f) Specific capacitance of PEDOT/MnO_2 (black), C-MnO_2 (red) and PEDOT/C-MnO_2 (blue) electrodes as a function of potential scan rate.

the PEDOT/C-MnO_2 electrode showed a higher current than the C-MnO_2 electrode at all the potential scan rates covered in this study. However, CV of the PEDOT/MnO_2 electrode became more distorted as the potential scan rate was increased from 5 mVs^{-1} to 100 mVs^{-1}. Furthermore, the PEDOT/MnO_2 electrode showed a smaller current than the C-MnO_2 electrode at the potential scan rates higher than 30 mVs^{-1}.

Figure 4(d) compares the specific capacitances of the three electrodes calculated from the CVs measured as a function of the potential scan rate. It should be noted that the PEDOT/C-MnO_2 electrode showed the highest specific capacitance and rate capability among the three electrodes. The specific capacitance of the PEDOT/C-MnO_2 electrode was 135 Fg^{-1} at 2 mVs^{-1} and it decreased to 98 Fg^{-1} at 100 mVs^{-1} with a capacitance loss of 28%.

The specific capacitances of the PEDOT/MnO_2 and C-MnO_2 electrodes were 135 and 101 Fg^{-1} at a low potential scan rate of 2 mVs^{-1}, respectively. The PEDOT/MnO_2 electrode showed a higher specific capacitance than the C-MnO_2 electrode at the low potential scan rates of 2 and 5 mVs^{-1}. As the potential scan rate was increased beyond 10 mVs^{-1}, however, the PEDOT/MnO_2 electrode showed a lower specific capacitance than the C-MnO_2 electrode. The specific capacitance of the PEDOT/MnO_2 was significantly decreased from 135 to 33 Fg^{-1} as the potential scan rate was increased from 2 to 100 mV/s^{-1} with a capacitance loss of 76%. On the contrary, the C-MnO_2 electrode showed a smaller capacitance loss 45% for the same potential scan rate increase, which indicates the better rate capability of the C-MnO_2 electrode compared with the PEDOT/MnO_2 electrode.

Analysis of Figure 4(d) from the view of the electrochemical utilization and rate capability of the active materials suggests that the PEDOT and conductive carbon in the composite electrodes have different roles in the composite electrodes. For the C-MnO_2 electrode, the conductive carbon mainly acted to provide a continuous conducting path from a current collector to MnO_2 particles in the electrode to improve the rate capability rather than the electrochemical utilization of the MnO_2. A limited number of active reaction sites of MnO_2 from the physical mixing of MnO_2 and the conductive carbon might be responsible for the poor electrochemical utilization of MnO_2. For the PEDOT/MnO_2 electrode, the conductive PEDOT layer on MnO_2 mainly acted to increase the number of active reaction sites of MnO_2 and thereby to improve the electrochemical utilization of the MnO_2 rather than the rate capability of the electrode. It has been reported that pure PEDOT electrode prepared without additional conductive carbon showed a poor rate capability.[24]

Thus, the higher electrochemical utilization and better rate capability of the PEDOT/C-MnO_2 electrode compared with those of the other two electrodes could be attributed to the increased number of active reaction provided by the PEDOT layer coated on MnO_2 and the continuous conducting path provided by the conductive carbon.

Conclusions

We have developed a facile route to the fabrication of PEDOT coated MnO_2 composite electrode by the galvanic displacement reaction. Analysis of cyclic voltammograms and specific capacitance of the composite electrodes suggests that the conductive carbon acts mainly to provide a continuous conducting path in the electrode to improve the

rate capability and the PEDOT layer on MnO_2 acts to increase the active reaction site of MnO_2.

Acknowledgments. This work was supported by Korea Science and Engineering Foundation (KOSEF) through the National Research Lab. Program funded by the Ministry of Education, Science and Technology (No. R0A-2007-000-10042-0) and a grant from the cooperative R&D Program (B551179-10-01-00) funded by the Korea Research Council Industrial Science and Technology, Republic of Korea.

References

1. Zhang, S. W.; Chen, G. Z. *Energy Materials: Materials Science and Engineering for Energy Systems* **2008**, *3*, 186.
2. Lee, H. Y.; Goodenough, J. B. *J. Solid State Chem.* **1999**, *144*, 220.
3. Toupin, M.; Brousse, T.; Belanger, D. *Chem. Mater.* **2002**, *14*, 3946.
4. Kim, H.; Popov, B. N. *J. Electrochem. Soc.* **2003**, *150*, D56.
5. Xie, X. F.; Gao, L. *Carbon* **2007**, *45*, 2365.
6. Yan, J.; Fan, Z. J.; Wei, T.; Qian, W. Z.; Zhang, M. L.; Wei, F. *Carbon* **2010**, *48*, 3825.
7. Kirchmeyer, S.; Reuter, K. *J. Mater. Chem.* **2005**, *15*, 2077.
8. Duay, J.; Gillette, E.; Liu, R.; Lee, S. B. *Phys. Chem. Chem. Phys.* **2012**, *14*, 3329.
9. Liu, R.; Lee, S. B. *J. Am. Chem. Soc.* **2008**, *130*, 2942.
10. Huang, Y. H.; Goodenough, J. B. *Chem. Mater.* **2008**, *20*, 7237.
11. Han, M. G.; Foulger, S. H. *Chem. Commun.* **2004**, 2154.
12. Ballav, N. *Mater. Lett.* **2004**, *58*, 3257.
13. Gemeay, A. H.; Mansour, I. A.; El-Sharkawy, R. G.; Zaki, A. B. *European Polymer Journal* **2005**, *41*, 2575.
14. Lee, W. R.; Kim, M. G.; Choi, J. R.; Park, J. I.; Ko, S. J.; Oh, S. J.; Cheon, J. *J. Am. Chem. Soc.* **2005**, *127*, 16090.
15. Xie, W.; Su, L.; Donfack, P.; Shen, A. G.; Zhou, X. D.; Sackmann, M.; Materny, A.; Hu, J. M. *Chem. Commun.* **2009**, 5263.
16. Pourbaix, M. *Atlas of Electrochemical Equilibria in Aqueous Solutions*, 1st English ed.; Pergamon Press: Oxford, New York, 1966.
17. Sakmeche, N.; Aaron, J. J.; Fall, M.; Aeiyach, S.; Jouini, M.; Lacroix, J. C.; Lacaze, P. C. *Chem. Commun.* **1996**, 2723.
18. Bobacka, J.; Lewenstam, A.; Ivaska, A. *J. Electroanal. Chem.* **2000**, *489*, 17.
19. Jiang, R. R.; Huang, T.; Liu, J. L.; Zhuang, J. H.; Yu, A. S. *Electrochim. Acta* **2009**, *54*, 3047.
20. Jean, F.; Cachet, C.; Yu, L. T.; Lecerf, A.; Quivy, A. *Journal of Applied Electrochemistry* **1997**, *27*, 635.
21. Julien, C. M.; Massot, M.; Poinsignon, C. *Spectrochim. Acta A* **2004**, *60*, 689.
22. Garreau, S.; Louarn, G.; Buisson, J. P.; Froyer, G.; Lefrant, S. *Macromolecules* **1999**, *32*, 6807.
23. Toupin, M.; Brousse, T.; Belanger, D. *Chem. Mater.* **2004**, *16*, 3184.
24. Kelly, T. L.; Yano, K.; Wolf, M. O. *Acs. Appl. Mater. Inter.* **2009**, *1*, 2536.